sciendo
DOI 10.2478/ama-2024-0079 *acta mechanica et automatica, vol.18 no.4 (2024)*

# SLIP BANDS AT THE TIPS OF NARROW SLOT IN BRAZILIAN NOTCHED DISK – PLANE DEFORMATION

**Andrzej KAZBERUK***

* Faculty of Mechanical Engineering, Bialystok University of Technology, ul. Wiejska 45A, 15-351 Bialystok, Poland

a.kazberuk@b.edu.pl

*received 04 November 2024, revised 07 November 2024, accepted 07 November 2024*

**Abstract:** Using the method of singular integral equations, the elastic-plastic problem for notched Brazilian disk at plane deformation state was solved. Based on Dugdale model the relationships between load, notch tip opening displacement and the length of the slip bands was established. The results demonstrate the potential of the proposed method for practical applications in engineering, particularly in the assessment of structural integrity under various loading conditions.

**Key words:** cracked Brazilian disk, Dugdale model, slip bands, plastic strips, plane deformation, singular integral equations

## 1. INTRODUCTION

The basic material parameter in fracture mechanics is the critical stress intensity factor, determined experimentally on specimens with initial cracks. In the case of metals, the procedure for determining this parameter is standardized and widely used. The fracture process, in this case, begins with a fatigue-initiated crack. For quasi-brittle materials such as concrete, ceramics, or rocks, it is difficult to obtain an initial crack with strictly defined parameters. Usually, the initial crack is produced during the specimen forming stage. In this way, slots of significant width (2-4 mm) with rounded tips are obtained.

Disk-type specimens are among the most commonly used test samples for determining Mode I and mixed-mode fracture toughness in brittle and quasi-brittle materials like ceramics, concrete, rocks, and rock-like materials. A circular disk specimen subjected to diametric compressive loading is a simple and well-established indirect testing method. These so-called Brazilian tests have been widely used to obtain the tensile strength of brittle materials. An up-to-date review of works concerning various aspects of the Brazilian test can be found in [10,17].

A disk with an internal central crack, as a convenient experimental specimen for testing fracture mechanics parameters, was considered analytically by [18,37-40]. These results concerning stress field distribution and values of the stress intensity factors were confirmed by [2,3,34].

Many recent works have been devoted to the investigation of the fracture process in brittle and quasi-brittle materials using compressed disks with central narrow slots. The papers [1,4,6,31,36] present experimental investigations of the critical value of the stress intensity factor under Mode I and Mode II loading conditions using various fracture criteria. It should be emphasized that the works cited above concern the problem of stress concentration in disk specimens with a strictly defined mathematical crack (i.e., a crack of zero width). The discussion of the influence of the relative crack length and the error of the loading angle on the experimental results for the Brazilian disk was presented by [8].

The semicircular disk with an edge narrow notch was also used as a test specimen [5,6].

Theoretical and experimental investigations have been performed for chevron-notched Brazilian disks [35], or for disks with multiple pre-existing notches [41].

The application of the deformation fracture criterion to the determination of basic fracture mechanics parameters requires knowledge of the relationship between the load level and the opening displacement at the crack tip. This means that, for an arbitrary test element, not only the stress field should be determined, but also the strain field, considering the changes taking place in the fracture process zone. General solutions for cracks or notches in an infinite plane are known ([23], see also [27]), but for particular specimens, these solutions can only be regarded as asymptotic.

In the paper [13], the solution for the elastic-plastic problem for notched Brazilian disks in a plane stress state was presented. Based on the Dugdale model [9,16] (see also [33], where this model is precisely described), and assuming that only one plasticity band emanates from the tip of the narrow slot placed at the center of the Brazilian disk, the relationships between load, notch tip opening displacement, and the length of the slip bands were established.

The aim of this work is similar to that of [13], i.e., to determine the relationship between the load level and the opening displacement at the tip of the narrow slot in a cylindrical specimen under diagonal compression, but in the plane strain state.

It is assumed that in the case of a plane strain state in a body with a sharp V-notch [15,30] or crack [14,19,21-23], the stress concentrator emits two slip bands that form a certain angle with respect to one another. We shall use this approach to solve the elastic-plastic problem for the notched Brazilian disk. We assume that the fracture process zone, characterized by plastic deformations near the vertices of the narrow slot in a perfectly elastic-plastic material under plane strain, localizes in two slip bands. Under symmetrical loading, these bands are simulated with cuts of unknown lengths, with the constant tangential stress equal to the shear yield limit in accordance with the Tresca-Saint Venant plasticity condition given at the cut edges. We suppose that normal displacements are

DOI 10.2478/ama-2024-0079

continuous at the contour cuts, while the tangential displacements exhibit a nonzero discontinuity at these contours.

## 2. PROBLEM FORMULATION

Consider a circular disk weakened by a narrow opening with vertices rounded by circular arcs of the radius $\rho$ (see Fig. 1a). The slot described by contour $L_1$ is placed at the disk center (contour $L_0$). Assume that the radius $R$ of circle $L_0$ is the unit length parameter. The projection of the slot onto the Ox axis measures $2l_1$=$2\gamma_1 R$. This indicates the total width of the slot. The contour of the slot consists of two parallel straight sections and two semicircles. The semicircles with radii $\rho$ form the vertices of the narrow slot [12,26,27]. The parameter $\varepsilon = \rho/l_1 = \rho/(\gamma_1 R)$ is the relative rounding radius of the slot vertices.

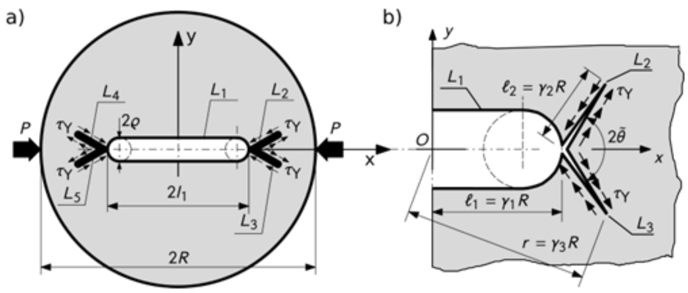


**Fig. 1.** a) Notched Brazilian disk with slip bands, b) detailed view on slot tip with emanating cracks

We assume that the fracture process zone is characterized by plastic deformations near the vertices of the narrow slot. In a perfectly elastic-plastic material subjected to plane strain, these deformations localize in two plastic bands, referred to as slip bands [21]. Under symmetrical loading, simulate these bands with cuts $L_2$, $L_3$ and $L_4$, $L_4$ of unknown lengths $l_2 = \cdots = l_5 = \ell_Y$ with the constant tangential stress $\tau_Y$ ($\tau_Y$ is shear yield limit in accordance with Tresca-Saint Venant plasticity condition $\tau_Y = \sigma_Y/2$) given at the cut edges. Suppose that normal displacements are continuous at contours $L_2$ and $L_3$ ($L_4$, $L_5$ respectively) while tangential displacements reveal a nonzero discontinuity at these contours.

These cuts with the contours $L_2$ to $L_5$) are symmetrically placed with respect to both axes of the Oxy system and inclined to the Ox axis at an angle $\theta$ (see Fig. 1b). The unknown relative extent of each linear defect that weakens the disk specimen is defined as $l_2 = \cdots = l_5 = \gamma_2 R$.

For the convenience of data composition in numerical calculations, an additional dimensionless geometric parameter $\gamma_3 = r/R$ is introduced. It defines the total distance of the slip band tip $r$ from the disk center.

The set of dimensionless geometric parameters $(\varepsilon, \gamma_1, \gamma_3)$ fully describes the domain under consideration. Assuming radius $R$ as basic unit length, we obtain relationships

$$l_1 = \gamma_1 R, \qquad l_2 = \cdots = l_5 = \gamma_2 R,$$
$$r = \gamma_3 R, \qquad \rho = \varepsilon l_1. \tag{1}$$

The value of the $\gamma_2$ parameter depends on the values of $\gamma_1$ and and $\gamma_3$:

$$\gamma_2 = \sqrt{\gamma_3^2 - \gamma_1^2 \sin^2\theta} - \gamma_1 \cos\theta. \tag{2}$$

Suppose that hole edge (the smooth contour $L_1$) is free of applied loads. The disk is loaded by two concentrated forces $P$, which compress the specimen along the Ox axis(Fig. 1a). Such type of loading cause concentration of tensile stresses in vertices ($\pm l_1$) of the hole.

The problem will be solved using singular integral equation method [25] (see also [27]). Complex stress potentials are written in the form [25]

$$\Phi_*(z) = \Phi_0(z) + \Phi(z),$$
$$\Psi_*(z) = \Psi_0(z) + \Psi(z), \tag{3}$$

where functions [20]:

$$\Phi_0(z) = \sigma_p \frac{z^2+R^2}{2(z^2-R^2)}, \ \Psi_0(z) = \frac{2R^4}{(z^2-R^2)^2}. \tag{4}$$

Nominal stress $\sigma_p = P/(\pi R)$ is equal to normal stress $\sigma_y$ alongside Ox axis, $z = x + iy$.

Functions $\Phi_0(z)$ and $\Psi_0(z)$ describe the stress state in a solid disk, which is a disk without any holes, loaded by concentrated forces. In contrast, the potentials $\Phi(z)$ and $\Psi(z)$ characterize the disturbed stress state caused by the opening ($L_1$) and the cuts ($L_2$ and $L_3$). These potentials are written in the following form [25]:

$$\begin{aligned}
\Phi(z) &= \frac{1}{2\pi}\int_L \left\{\left[\frac{1}{t-z} + \frac{\bar{t}}{z\bar{t}-R^2}\right] g'(t)dt + \right. \\
&\quad \left. + \frac{z(t\bar{t}-R^2)(z\bar{t}-2R^2)}{R^2(z\bar{t}-R^2)^2}\overline{g'(t)}d\bar{t}\right\}, \\
\Psi(z) &= \frac{1}{2\pi}\int_L \left\{\left[\frac{\bar{t}^3}{(z\bar{t}-R^2)^2} - \frac{\bar{t}}{(t-z)^2}\right] g'(t)dt + \right. \\
&\quad \left. + \left[\frac{1}{t-z} + \frac{\bar{t}}{z\bar{t}-R^2} + \frac{\bar{t}(z\bar{t}-3R^2)(t\bar{t}-R^2)}{(z\bar{t}-R^2)^3}\right]\overline{g'(t)}d\bar{t}\right\}.
\end{aligned} \tag{5}$$

Here $g'(t)$ ($t \in L_k$, $k$=1, ... ,5) is an unknown function of the derivative of displacement discontinuity vector across the cut contour.

The boundary condition at the contour $L$ is expressed as follows:

$$N(t) + iT(t) = p(t) \quad t \in L, \quad L = \cup_{k=1}^{5} L_k, \tag{6}$$

where $N$ and $T$ are normal and tangential components of the stress vector. The right side of the equation (6) is equal [25]

$$p(t) = \sigma_k - \left\{\Phi_0(t) + \overline{\Phi_0(t)} + \frac{d\bar{t}}{dt}\left[t\overline{\Phi_0'(t)} + \overline{\Psi_0(t)}\right]\right\},$$
$$t \in L, \tag{7}$$

It was assumed that constant tangential stress is equal $\tau_Y = \sigma_Y/2$. Where $\sigma_Y$ is equal to the material strength of the specimen

DOI 10.2478/ama-2024-0079 acta mechanica et automatica, vol.18 no.4 (2024)

determined in the Brazilian test (compressed disk without slot):

$$\sigma_k = \begin{cases} 0, & k = 1, \\ i\tau_Y, & k = 2, \dots, 5 \end{cases} \tag{8}$$

Fulfilling boundary condition 6) using potentials (5) we obtain the system of singular integral equations with unknown functions $g'_m(t)$ ($m$=1, … ,5)

$$\frac{1}{\pi}\sum_{k=1}^{3}\int_{L_k}\left[K_{km}(t,t')g'_m(t)dt + L_{km}(t,t')\overline{g'_m(t)}d\bar{t}\right] = p_m(t'), \qquad t' \in L_m, \quad m = 1,\dots,5, \tag{9}$$

where kernels are as follows:

$$K(t,t') = f_1(t,t') + \overline{f_2(t,t')} + \frac{d\overline{t'}}{dt}\left[t'\overline{g_2(t,t')} + \overline{h_2(t,t')}\right], \tag{10}$$

$$L(t,t') = f_2(t,t') + \overline{f_1(t,t')} + \frac{d\overline{t'}}{dt}\left[t'\overline{g_1(t,t')} + \overline{h_1(t,t')}\right], \tag{11}$$

where

$$f_1(t,t') = \frac{1}{2}\left[\frac{1}{t-t'} + \frac{\bar{t}}{t'\bar{t}-R^2}\right], \tag{12}$$

$$f_2(t,t') = \frac{t'(t\bar{t}-R^2)(t'\bar{t}-2R^2)}{2R^2(t'\bar{t}-R^2)^2}, \tag{13}$$

$$g_1(t,t') = \frac{1}{2}\left[\frac{1}{(t-t')^2} - \frac{\bar{t}^2}{(t'\bar{t}-R^2)^2}\right], \tag{14}$$

$$g_2(t,t') = \frac{R^2(t\bar{t}-R^2)}{(t'\bar{t}-R^2)^3}, \tag{15}$$

$$h_1(t,t') = \frac{1}{2}\left[-\frac{\bar{t}}{(t-t')^2} + \frac{\bar{t}^3}{(t'\bar{t}-R^2)^2}\right], \tag{16}$$

$$h_2(t,t') = \frac{1}{2}\left\{\frac{1}{t-t'} + \frac{\bar{t}\left[4R^4 - 3R^2\bar{t}(t'+t) + t'\bar{t}^2(t'+t)\right]}{(t'\bar{t}-R^2)^3}\right\}. \tag{17}$$

## 3. NUMERICAL SOLUTION OF SINGULAR INTEGRAL EQUATIONS

Assume clockwise direction of tracing the contour $L_1$ so the elastic region stays on the left during tracing. Taking into consideration symmetry of the contour with respect to both coordinate axes, we can write its parametric equation in the form [27]:

$$t = R\omega_1(\xi) = R\begin{cases} \omega_q(\xi), & 0 \le \quad \xi \quad \pi/2, \\ -\overline{\omega_q(\pi-\xi)}, & \pi/2 \le \quad \xi \quad \pi, \\ -\omega_q(\xi-\pi), & \pi \le \quad \xi \quad <3\pi/2, \\ \overline{\omega_q(2\pi-\xi)}, & 3\pi/2 \le \quad \xi \quad <2\pi. \end{cases} \tag{18}$$

the function $\omega_q(\xi)$ describes the segment of contour $L_1$ laying in the fourth quarter of the coordinate system:

$$\omega_q(\xi) = \begin{cases} 1-\varepsilon+\varepsilon(\cos c\xi - i\sin c\xi), & 0 \le \quad \xi \quad \pi/(2c), \\ \varepsilon c(\pi/2-\xi) - i\varepsilon, & \pi/(2c) \le \quad \xi \quad \pi/2, \end{cases} \tag{19}$$

where parameter $c$=$1 + 2(1/\varepsilon - 1)/\pi$. Total contour $L_1$ length equals to $2\pi\varepsilon\gamma_1$Rc.

Parametric equation describing cut $L_2$ is written in the form

$$t = R\omega_2(\xi) = R\left[\gamma_1 + \frac{1}{2}\gamma_2(1+\xi)e^{i\theta}\right], -1 \le \xi \le 1 \tag{20}$$

Contour $L_3$ is symmetrical to $L_2$ with respect to the Ox axis so

$$t = R\omega_3(\xi) = R\overline{\omega_2(\xi)}, -1 \le \xi \le 1. \tag{21}$$

Contours $L_4$ and $L_5$ are symmetrical to $L_2$ and $L_3$ with respect to the Oy axis so

$$t = R\omega_4(\xi) = -R\overline{\omega_2(\xi)}, t = R\omega_5(\xi) = -R\omega_2(\xi), \quad -1 \le \xi \le 1 \tag{22}$$

Introducing substitutions

$$t = R\omega_1(\xi), t' = R\omega_1(\eta), t,t' \in L_1, 0 \le \xi,\eta \le 2\pi,$$
$$t = R\omega_k(\xi), t' = R\omega_k(\eta), t,t' \in L_k,$$
$$k=2,\dots,5, -1 \le \xi,\eta \le 1, \tag{23}$$

one can reduce the system of integral equations (9) to the canonical form

$$\frac{1}{\pi}\int_0^{2\pi}\left[M_{1m}(\xi,\eta)g'_1(\xi) + N_{1m}(\xi,\eta)\overline{g'_1(\xi)}\right]d\xi + \frac{1}{\pi}\sum_{k=2}^{5}\int_{-1}^{1}\left[M_{km}(\xi,\eta)g'_k(\xi) + N_{km}(\xi,\eta)\overline{g'_k(\xi)}\right]d\xi = p_m(\eta), m = 1,2,3, \tag{24}$$

where

$$M_{\mathrm{km}}(\xi,\eta) = RK_{\mathrm{km}}(R\omega_k(\xi), R\omega_m(\eta)), \tag{25}$$

$$N_{\mathrm{km}}(\xi,\eta) = RL_{\mathrm{km}}(R\omega_k(\xi), R\omega_m(\eta)), \tag{26}$$

$$g'_k(\xi) = g'(R\omega_k(\xi))\omega'_k(\xi), \tag{27}$$

$$p_m(\eta) = p(R\omega_m(\eta)). \tag{28}$$

A solution of the system of integral equations (24) consists of five complex functions $g'_k(\xi)$ assigned to the contours $L_k$. Function $g_1(\xi)$ ($0 \le \xi \le 2\pi$) is $2\pi$--periodic continuous function. However, in order to obtain a sufficiently accurate numerical solution we have to densify quadrature nodes and collocation points in the vicinity of narrow slot tips. We use here nonlinear variant of sigmoid transformation [11,32] adapted to periodic case [32]:

$$\xi = G(\tau) = \tau - \frac{1}{2}\sin 2\tau, 0 \le \tau \le 2\pi. \tag{29}$$

Consequently, the function we are looking for is as follows

$$u_1(\tau) = g'_1(G(\tau)), 0 \le \tau \le 2\pi. \tag{30}$$

A solution of the system of integral equations (24) for contours $L_2$ to $L_5$ is sought in the class of functions, which have an integrable singularity at the ends of integration interval

$$g'_k(\xi) = \frac{u_k(\xi)}{\sqrt{1-\xi^2}}, -1 \le \xi \le 1, \tag{31}$$

where $u_k(\xi)$ ($k$=2, … ,5) are continuous functions. Finally, modified system of singular integral equation (24) takes the form

$$\frac{1}{\pi}\int_0^{2\pi}\left[M_{1m}(\xi,\eta)u_1(\tau) + N_{1m}(\xi,\eta)\overline{u_1(\tau)}\right]G(\tau)d\tau + \frac{1}{\pi}\sum_{k=2}^{5}\int_{-1}^{1}\left[M_{km}(\xi,\eta)u_k(\xi) + N_{km}(\xi,\eta)\overline{u_k(\xi)}\right]d\xi = p_m(\eta), m = 1,2,3 \tag{32}$$

In points $t = \pm l_1$ where contours $L_2$ to $L_5$ intersect contour $L_1$ the values of $g'_k(-1)$ ($k$=2,5) must be finite, thus we should provide four additional equations

$$u_k(-1)=0, k=2,5. \tag{33}$$

For numerical integration of singular integral equation (32) two different methods must be used. For closed-loop contour $L_1$, we applay midpoint rule [7] and Gauss-Chebyshev quadrature [25] for $L_2$ to $L_5$ contours. Finally, we get a system of complex linear algebraic equations which is the discrete analogue of the respective system of integral equations (24)

DOI 10.2478/ama-2024-0079

$$\frac{2}{n_1}\sum_{i=1}^{n_1}\left[M_{1m}(\xi_i,\eta_j)u_1(\tau_i)+N_{1m}(\xi_i,\eta_j)\overline{u_1(\tau_i)}\right]G(\tau_i)+\sum_{k=2}^{5}\left\{\frac{1}{n_k}\sum_{i=1}^{n_k}\left[M_{km}(\xi_i,\eta_j)u_k(\xi_i)+N_{km}(\xi_i,\eta_j)\overline{u_k(\xi_i)}\right]\right\}=p_m(\eta_j), \tag{34}$$

$m=1,\quad j=1,\dots,n_k,\ m=2,\dots,5,\quad j=1,\dots,(n_k-1)$

where quadrature nodes and collocation points are determined by the formulas:

$$\xi_i=G(\tau_i),\tau_i=\frac{\pi(2i-1)}{n_1}, i{=}1,\dots,n_1, \tag{35}$$

$$\eta_j=G(\theta_j),\theta_j=\frac{2\pi(j-1)}{n_1}, j{=}1,\dots,n_1, \tag{36}$$

$$3\xi_i=\cos\frac{\pi(2i-1)}{2n_k}, i{=}1,\dots,n_k, k{=}2,\dots,5, \tag{37}$$

$$\eta_j=\cos\frac{\pi j}{n_k}, j{=}1,\dots,(n_k-1), k{=}2,\dots,5. \tag{38}$$

Assuming $n_2=n_3=\dots=n_5$ the system (34) consists of $n_1+4(n_2-1)$ complex equations. Using Lagrange interpolation on Chebyshev nodes [25] to conditions (33), we obtain four missing equations

$$\frac{1}{n_k}\sum_{i=1}^{n_k}\quad(-1)^{i+n_k}\tan\frac{\pi(2i-1)}{4n_k}u_k(\xi_i)=0,\quad k=2,\dots,5. \tag{39}$$

Right side of the equation (34) can be easily calculated using relationship (7). Introducing the relation $\gamma_Y=\sigma_p/\tau_Y$ ($\sigma_p=P/(\pi R)$) as relative load level parameter, we can write down $p_m(\eta_j)$ in compact form:

$$p_m(\eta_j)=\begin{cases}p_1(\eta_j), & m=1,\\ \left(1-\frac{i}{\gamma_Y}\right)p_1(\eta_j), & m=2,\dots,5,\end{cases} \tag{40}$$

where

$$p_1(\eta_j)=\sigma_p\frac{|\omega_k(\eta_j)|^2-1}{\overline{\omega_k(\eta_j)}^2-1}\left[\frac{2}{\overline{\omega_k(\eta_j)}^2-1}\frac{\overline{\omega_k'(\eta_j)}}{\omega_k'(\eta_j)}-\frac{|\omega_k(\eta_j)|^2+1}{\omega_k(\eta_j)^2-1}\right],\quad k{=}1,\dots,5. \tag{41}$$

Solution of the problem is symmetrical with respect to the axis *Ox* i *Oy*. Conditions resulting from symmetry concerning the sought function $u_k(\xi)$ and necessary kernel modifications are described in details in [29] (see also [27]). Thus, the rank of linear system (34), (39), can be easily reduce by a factor of four.

Having obtained values of sought function $u(\xi_k)$, one can determine the stress-strain state in whole elastic region by using an integral representation of complex stress potentials (5).

The slot edge (contour $L_1$) is free of applied load, then the contour stress at the edge can be calculated using a simple formula [27].

$$\sigma_s=-4\sigma_p\Im\frac{u_1(\xi)}{\omega_1'(\xi)}=-4\sigma_p\Im\frac{u_1(\tau)}{\omega_1'(G(\tau))}. \tag{42}$$

Stress intensity factors in crack tips $K_I$ and $K_{II}$ can be directly expressed through the sought function $g_k'(t)$ (31). Let us introduce corresponding dimensionless stress intensity factors $F_I$ and $F_{II}$ by means of the following relationship

$$K_I^+-iK_{II}^+=(F_I^+-iF_{II}^+)\sigma_p\sqrt{\pi R}. \tag{43}$$

Here upper indexes $(+)$ indicate crack tip at $\xi=+1$. Taking into account relation (31), we get for coefficients $F_I$ and $F_{II}$ the formula [25]:

$$F_I^+-iF_{II}^+=-\sqrt{|\omega_k{}'(+1)|}\frac{u_k(+1)}{\omega_k{}'(+1)},\quad k=2,\dots,5, \tag{44}$$

where

$$u_k(+1)=-\frac{1}{n}\sum_{i=1}^{n_k}\quad(-1)^i u_k(\xi_i)\cot\frac{\pi(2i-1)}{4n},\quad k=2,\dots,5. \tag{45}$$

Cracks $L_2$ and $L_3$ (and $L_4$, $L_5$ respectively) simulate fracture process zones (slip bands) at the tips of narrow slot $L_1$, thus stresses at the crack $L_k$ end must be finite

$$g_k'(t=\pm(l_k))=g_k'(R\omega_k(+1)){=}0,\rightarrow u_k(+1){=}0, k{=}2,\dots,5. \tag{46}$$

This condition allows as to calculate unknown length $l_2=\gamma_2 R$ using iteration process.

The length of slip band depends on the value of the angle $\theta$. It was assumed that there is an unique $\theta$ angle for which the band length is maximum.

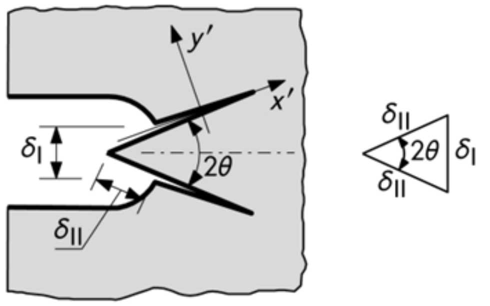


**Fig. 2** Slot tip opening displacement

Opening displacement at the notch tip (Fig. 2) can be calculated based on known [25] relationship between function $g_k(t)$ ($k$=2,3) and displacement discontinuity vector $(v_k^+-v_k^-)$ across the contour $L_k$

$$2G\frac{d}{dx'}(v_k^+-v_k^-)=(1+\kappa)g_k'(x'),\qquad x'\in L_k,\quad k=2,\dots,5, \tag{47}$$

where $x'$ is a local abscissa at contour $L_k$, $G$ - shear modulus, $\kappa$ - Muskhelishvili's constant.

Taking into consideration that in the beginning of cuts $L_2$ and $L_3$ only tangential displacements have discontinuity $\delta_{II}$, we obtain (see Fig. 2)

$$\delta_I^V{=}2\delta_{II}\sin\theta. \tag{48}$$

The relationship $(1+\kappa)/(4G){=}2(1-\nu^2)/E$ is valid in plane strain state, so taking into account (47), one can find the tangential displacement across cut edges $Ł_2=$ in the point $x'=l_2^-$, i.e. in the slot tip, as follows

$$\delta_{II}=\Im\delta(l_2^-)=\frac{4(1-\nu^2)}{E}\Im g(l_2^-), \tag{49}$$

where values of function $g(l_2^-)$ are determined by relationship (45):

$$\tilde{\delta}_I=-\frac{8(1-\nu^2)}{E}\sin\theta\frac{1}{n_2}\sum_{i=1}^{n_2}\quad\Im u_2(\xi_i). \tag{50}$$

In the next section the relationship between the theoretical value of dimensionless notch tip opening displacement $\tilde{\delta}_I$ and critical load value $\sigma_c=\sigma_n$ for given geometrical parameters (narrow slot tip radius $\varepsilon$, relative slot range $\gamma_1$), and standard material constants (Young's modulus $E$, Poisson's ratio $\nu$, relative material strength $\gamma_Y$). Knowing the value of the critical load the critical stress intensity factor $K_c$ can be calculated with the following formula 23,24]:

$$K_c = \sqrt{\delta_I E \sigma_c} = \sqrt{\tilde{\delta}_I \gamma_Y} \sigma_c \sqrt{\pi R}. \quad (51)$$

## 4. NUMERICAL RESULTS

The problem as it was stated have two independent geometrical parameters: $\varepsilon$, $\gamma_1$, and dimensionless load level $\gamma_Y$. The unknown are relative band length $\gamma_2$ (or extent $\gamma_3$) and the angle $2\theta$ between bands which emanates from slot tip. In order to reduce the number of independent parameters, it was assumed constant rounding radius of slot tips $\rho$=1/75$R$ and the calculations were performed for the relative slot span $\gamma_1$ chosen from the set $\gamma_1 = \{0.1,0.2,0.3,0.4,0.5\}$, thus relative rounding radius of the slot vertices can be easily calculated as $\varepsilon$=1/(75$\gamma_1$).

As has been shown in [13,27], plastic deformation near rounded notch tip begins when tangential stresses $\tau_n$ at lines directed along slip bands reach half of the maximal normal stress $(\sigma_s)_{\max}$ value. Which lets you calculate corresponding minimal load level $(\gamma_Y)_{\min}$

$$|\tau_n|_{\max} = \tau_Y = \frac{1}{2}(\sigma_s)_{\max} \to (\gamma_Y)_{\min} = \frac{2}{R_I} \approx 0.668. \quad (52)$$

The value of the stress rounding factor [26,28] is $R_I$=2.992.

The following discrete set of $\gamma_Y = \sigma_p/\tau_Y$ values was used for calculations: $\gamma_Y = [0.8, 0.9, 1.0, 1.2, 1.5, 2.0, 5.0]$. The $\theta$ values were taken from the $1^\circ \le \theta \le 85^\circ$ range every 5 degrees, decreasing the step in the vicinity of the sought maximum value of $\gamma_2$.

Fig. 3 shows the dependence of the $\gamma_3$ range on the slip band angle $\theta$ for several loading levels $\gamma_Y$. As can be seen, for the minimum $\gamma_Y$=0.8 value the maximum range of the bands is achieved for an angle of approximately $\theta$=2.3° with a corresponding range of $\gamma_3$=0.89. For higher values of the load level $\gamma_Y$ the maxima of the function $\gamma_3(\theta)$ shift towards $\theta \to 0$.

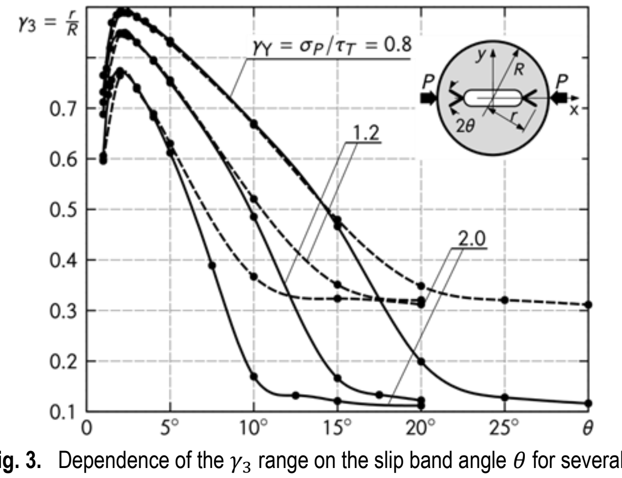


**Fig. 3.** Dependence of the $\gamma_3$ range on the slip band angle $\theta$ for several loading levels $\gamma_Y$.

The dependence of the relative length of the slip band $\gamma_2$ on the narrow slot extent $\gamma_1$ is shown in Fig. 4. For longer slots the $\gamma_2(\gamma_Y)$ bandwidth functions become less and less predictable.

Fig. 5 shows the plot of the $\delta_I$ notch tip opening displacemnt dependence on the $\gamma_Y$ load level for several values of the central slot range $\gamma_1$.

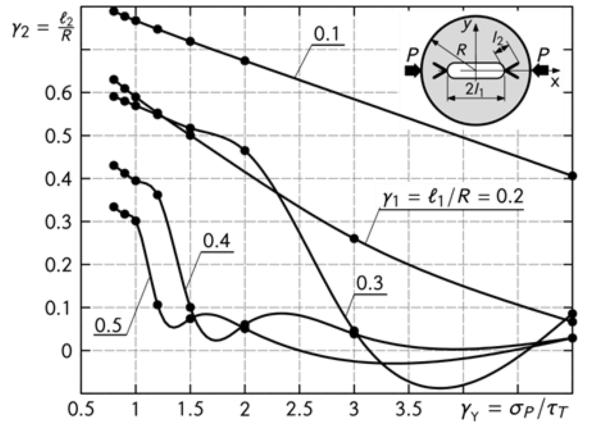


**Fig. 4.** Dependence of the relative length of the slip band $\gamma_2$ on the narrow slot extent $\gamma_1$

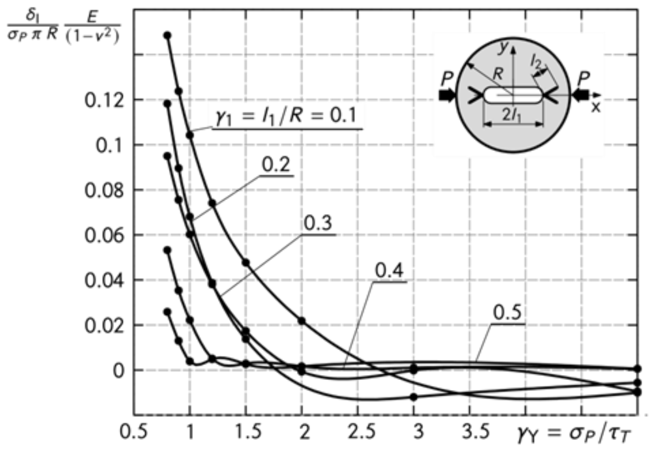


**Fig. 5.** Notch tip opening displacement $\delta_I$ dependence on the $\gamma_Y$ load level for several values of the central slot range $\gamma_1$

## 5. CONCLUSIONS

The elastic-plastic problem for Brazilian disk with central narrow slot in plane strain state was solved. The solution was obtained by the method of singular integral equations with complex stress potentials for a system of cracks and openings in two-dimensional circular elastic domain. All necessary analytical background was documented in detail. Based on Dugdale model of fracture process zone, relationships between the load, notch tip opening displacement, and the length of the slip bands were established. Numerical calculations for arbitrary but representative set of geometrical parameters were performed.

The presented solution, despite the obvious simplifications resulting from the adopted assumptions (plane strain state and fracture process zone as a slip band), can be used to estimate the fracture mechanics parameters of quasi-brittle materials determined in the Brazilian test.

## REFERENCES

1. Atahan HN, Tasdemir MA, Tasemir C, Ozyurt N and Akyuz S. Mode I and mixed mode fracture studies in brittle materials using the Brazilian disc specimen. Mater. Struct. 2005; 38:305–12.
2. Atkinson C, Smelser R, and Sanchez J. Combined mode fracture via the cracked Brazilian disk test. Int. J. Fract. 1982;18:279–91.
3. Awaji H and Sato S. Combined mode fracture toughness measurement by the disk test. J.Eng. Mater. Technol. 1978;100:175–82.

DOI 10.2478/ama-2024-0079

4. Ayatollahi M, Aliha M. Mixed mode fracture in soda lime glass analyzed by using the generalized MTS criterion. International Journal of Solids and Structures 2009; 46:311–21.
5. Ayatollahi M and Aliha M. On the use of Brazilian disc specimen for calculating mixed mode I–II fracture toughness of rock materials. Engineering Fracture Mechanics 2008;75:4631–41.
6. Ayatollahi M, Aliha M. Wide range data for crack tip parameters in two disc-type specimens under mixed mode loading. Computational Materials Science 2007;38:660–70.
7. Belotserkovsky SM and Lifanov IK. Method of discrete vortices. CRC Press LLC. Boca Raton. 1993.
8. Dong S. Theoretical analysis of the effects of relative crack length and loading angle on the experimental results for cracked Brazilian disk testing. Engineering Fracture Mechanics 2008;75:2575–81.
9. Dugdale D. Yielding of steel sheets containing slits. J. Mech. Phys. Solids 1960; 8:100–4.
10. Garcı́a VJ, Márquez CO, Zúñiga-Suárez AR, Zuñiga-Torres BC, Villalta-Granda LJ. Brazilian Test of Concrete Specimens Subjected to Different Loading Geometries: Review and New Insights. International Journal of Concrete Structures and Materials. 2017;11:343–63.
11. Johnston PR. Application of sigmoidal transformations to weakly singular and near-singular boundary element integrals. Int. J. Numer. Meth. Eng. 1999; 45:1333–48.
12. Kazberuk A. Koncentracja naprężeń wokół owalnego otworu. Acta Mech. Autom. 2007;1:25–30.
13. Kazberuk A. Application of the Deformation Fracture Criterion to Cracking of Disc Specimens with a Central Narrow Slot. Acta Mechanica et Automatica. 2022;16.
14. Kipnis LA, Cherepanov GP. Slip lines at the vertex of a wedge-like cut. J. Appl. Math. Mech. 1984; 48:112–4.
15. Kuliev VD. Plastic rupture lines at the tip of a wedge. Int. Appl. Mech. 1979; 15:221–7.
16. Leonov MY, Panasyuk VV. Development of a nanocrack in a solid. Prikl. Mekh. 1959; 5:391–401.
17. Li D, Wong LNY. The Brazilian disc test for rock mechanics applications: review and new insights. Rock mechanics and rock engineering 2013; 46:269–87.
18. Libatskii L, Kovchik S. Fracture of discs containing cracks. Mater. Sci. 1967; 3:334–9.
19. Lo KK. Modeling of plastic yielding at a crack tip by inclined slip planes. Int. J. Fract. 1979; 15:583–9.
20. Muskhelishvili NI. Some Basic Problems of the Mathematical Theory of Elasticity. Foundamental Equations Plane Theory of Elasticity Torsion and Bending. 2nd ed. Noordhoff International Publishing, Leyden. 1977:764.
21. Panasyuk VV, Savruk MP. Model for plasticity bands in elastoplastic failure mechanics. Mater. Sci. 1992; 28:41–5.7
22. Panasyuk VV, Savruk MP. Plastic strip model in elastic-plastic problems of fracture mechanics. Adv. Mech 1992; 15:123–47.
23. Rice JR. Limitations to the small scale yielding approximation for crack tip plasticity. J. Mech. Phys. Solids 1974; 22:17–26.
24. Rice JR. The location of plastic deformation. Theor. Appl. Mech. 1976; 1:207–20.
25. Savruk MP. Two-dimensional problems of elasticity for bodies with cracks (in Russian). Naukova Dumka. Kiev. 1981.
26. Savruk MP, Kazberuk A. A unified approach to problems of stress concentration near V-shaped notches with sharp and rounded tip. Int. Appl. Mech. 2007; 43:182–97.
27. Savruk MP, Kazberuk A. Stress Concentration at Notches. Springer International Publishing Switzerland. 2017;498.
28. Savruk MP, Kazberuk A. Two-dimensional fracture mechanics problems for solids with sharp and rounded V-notches. Int. J. Fract. 2010; 161:79–95.
29. Savruk MP, Osiv PN, Prokopchuk IV. Numerical analysis in plane problems of the crack theory (in Russian). Naukova Dumka, Kiev. 1989.
30. Savruk MP, Zavodovs'kyi AM, Panasyuk VY. On fracture of bodies with V-notches under plane strain. Mekhanika i fizyka ruinuvannya budivelnykh materialiv ta konstruktsii (Mechanics and physics of fracture of building materials and structures). Lviv. 2005;10:140–7.
31. Seitl S, Miarka P. Evaluation of mixed mode I/II fracture toughness of C 50/60 from Brazilian disc test. Frattura ed Integrità Strutturale 2017; 11:119–27
32. Sidi A. A new variable transformation for numerical integration. H. Brass H. and G. Hämmerlin, editors. Numerical integration IV. Ed. by Brass H and Hämmerlin G. 1993;359–73.
33. Sun CT. Fracture mechanics. Ed. by Jin ZH. Waltham. Mass. Butterworth-Heinemann/Elsevier. 2012;311 pp.
34. Tang S. Stress intensity factors for a Brazilian disc with a central crack subjected to compression. International Journal of Rock Mechanics and Mining Sciences 2017; 93:38–45.
35. Wang Q, Gou X, Fan H. The minimum dimensionless stress intensity factor and its upper bound for CCNBD fracture toughness specimen analyzed with straight through crack assumption. Engineering Fracture Mechanics 2012; 82:1–8.
36. Xiankai B, Meng T, Jinchang Z. Study of mixed mode fracture toughness and fracture trajectories in gypsum interlayers in corrosive environment. Royal Society Open Science. 2018; 5.
37. Yarema SY, Ivanitskaya G, Maistrenko A, Zboromirskii A. Crack development in a sintered carbide in combined deformation of types I and II. Strength of Materials 1984; 16:1121–8.
38. Yarema SY. Stress state of disks with cracks, recommended as specimens for investigating the resistance of materials to crack development. Mater. Sci. 1977;12:361–74.
39. Yarema SY and Krestin GS. Determination of the modulus of cohesion of brittle materials by compressive tests on disc specimens containing cracks. Mater. Sci. 1967; 2:7–10.
40. Yarema SY, Krestin GS. Limiting equilibrium of a disk with a diametral crack. Int. Appl. Mech. 1968; 4:55–8.
41. Zhou S. Fracture Propagation in Brazilian Discs with Multiple Pre-existing Notches by Using a Phase Field Method. Periodica Polytechnica Civil Engineering 2018; 62:700–8.

The work has been accomplished under the research project No. WZ/WM-IIM/3/2020.

Andrzej Kazberuk: https://orcid.org/0000-0003-4179-0312